

## **General Disclaimer**

### **One or more of the Following Statements may affect this Document**

- This document has been reproduced from the best copy furnished by the organizational source. It is being released in the interest of making available as much information as possible.
- This document may contain data, which exceeds the sheet parameters. It was furnished in this condition by the organizational source and is the best copy available.
- This document may contain tone-on-tone or color graphs, charts and/or pictures, which have been reproduced in black and white.
- This document is paginated as submitted by the original source.
- Portions of this document are not fully legible due to the historical nature of some of the material. However, it is the best reproduction available from the original submission.

**NASA TECHNICAL  
MEMORANDUM**

NASA TM X-71601

NASA TM X-71601



EARLY OPERATION EXPERIENCE ON THE ERDA/NASA  
100 kW WIND TURBINE

by John C. Glasgow and Bradford S. Linscott  
Lewis Research Center  
Cleveland, Ohio  
September 1976

(NASA-TM-X-71601) EARLY OPERATI N  
EXPERIENCE ON THE ERDA/NASA 100 kW WIND  
TURBINE (NASA) 25 p HC A02/MF A01 CSCL 10A

N77-10640

Unclas  
G3/44 08948

1. Report No. <b>NASA TM X-71601</b>		2. Government Accession No.		3. Recipient's Catalog No.	
4. Title and Subtitle <b>EARLY OPERATION EXPERIENCE ON THE ERDA/NASA 100 kW WIND TURBINE</b>				5. Report Date	
				6. Performing Organization Code	
7. Author(s) <b>John C. Glasgow and Bradford S. Linscott</b>				8. Performing Organization Report No. <b>E-8076</b>	
9. Performing Organization Name and Address <b>Lewis Research Center National Aeronautics and Space Administration Cleveland, Ohio 44135</b>				10. Work Unit No.	
				11. Contract or Grant No.	
12. Sponsoring Agency Name and Address <b>National Aeronautics and Space Administration Washington, D.C. 20546</b>				13. Type of Report and Period Covered <b>Technical Memorandum</b>	
				14. Sponsoring Agency Code	
15. Supplementary Notes					
16. Abstract <p>As part of the Energy Research and Development Administration (ERDA) wind-energy program, NASA Lewis Research Center is testing an experimental 100-kW wind turbine at Sandusky, Ohio. Rotor-blade and drive-shaft loads and tower deflection were measured during operation of the wind turbine at rated rpm. The blade loads measured are higher than anticipated. Preliminary results indicate that air-flow blockage by the tower structure probably causes the high rotor-blade-bending moments.</p>					
17. Key Words (Suggested by Author(s)) <b>Wind turbines, Computer simulation, Aerodynamic loads, Wind tunnel tests Structural mechanics, Dynamic response,</b>			18. Distribution Statement <b>STAR category 44 Unclassified - unlimited</b>		
19. Security Classif. (of this report) <b>Unclassified</b>		20. Security Classif. (of this page) <b>Unclassified</b>		21. No. of Pages	22. Price*

\* For sale by the National Technical Information Service, Springfield, Virginia 22161

## EARLY OPERATION EXPERIENCE ON THE ERDA/NASA 100 kW

### WIND TURBINE

By John C. Glasgow and Bradford S. Linscott

National Aeronautics and Space Administration  
Lewis Research Center  
Cleveland, Ohio 44135

### INTRODUCTION

The 100 kW Experimental Wind Turbine is a part of the national wind energy program under the direction of the Energy Research and Development Administration (ERDA). The NASA Lewis Research Center has designed, built and erected this machine near Sandusky, Ohio, and is currently testing it to obtain engineering data on large horizontal axis wind turbines.

The wind turbine has a 125 foot diameter two-bladed rotor (ref. 1) which drives a 100 kW capacity synchronous generator through a step-up gear box. The rotor is positioned downwind of a 100-foot steel truss tower as pictured in Figure 1. The rotor is designed to operate at a constant speed of 40 rpm, and it drives a 480 volt 60 hz three-phase generator at 1800 rpm. Constant rotor speed is maintained by controlling the blade pitch angle with an active feedback control system. The rotor, generator, transmission and associated equipment are mounted in a nacelle, Figure 2, which can be yawed to align the rotor with the wind. Power, instrumentation and control connections to the ground are made through slip rings.

The turbine was designed to begin generating power in winds of 10 mph (100 feet), and produce 100 kW at a wind velocity of 18 mph. In winds above 18 mph, the generator continues to operate at a 100 kW output by adjusting the pitch of the rotor to spill the excess wind energy. When the wind velocity exceeds 40 mph, the blades are feathered to bring the rotor to a stop in a horizontal position. A brake is then applied at the high-speed drive shaft to lock the rotor blades against rotation.

Final assembly of the machine was completed in September 1975 (ref. 2), and it became operational in October. In December 1975 the machine first achieved its design speed of 40 rpm and produced 100 kW of power. During the course of these initial operations, data was taken on the rotor, blades, the nacelle and the tower. Some of this data describes the coupled dynamic response of the machine. Selected portions of this data are presented and discussed in this report, along with a brief description of the instrumentation.

E-807E

## INSTRUMENTATION

The 100 kW wind turbine data system provides approximately 100 channels of real-time continuous information. Some of this data is discussed below.

1. Wind velocity and azimuth from a meteorological tower.
2. Wind velocity and nacelle yaw angle relative to the wind, from the wind turbine nacelle as shown in Figure 1.
3. Tower deflections  $x$  and  $y$ .
4. Nacelle accelerations  $x$ ,  $y$  and  $z$  at the rotor shaft bearing support nearest to the rotor.
5. Rotor blade pitch angle.
6. Rotor blade bending moments, indicating beamwise ( $M_m$ ) and chordwise ( $M_n$ ) bending at two stations along the blade span.
7. Rotor shaft torque ( $M_z$ ) and bending moments  $M_x$  and  $M_y$ .
8. Rotor speed and blade position.
9. Alternator output.

Figures 3 and 4 give a schematic representation of these measurements, their location on the wind turbine, and the sign convention of each. The data reported herein were taken on strip chart recorders. Composites of this data is shown in Figures 5a through 8d. Each set of data is time correlated, the  $T_1$  and  $T_2$  lines referring to the same instant of time from chart to chart. The time in seconds and the time when blade #1 passes through the  $290^\circ$  point is indicated on the top and bottom of each data figure.

## DISCUSSION OF TEST DATA

### Design Speed at Rated Power

The measured moment data shown in Figures 5a, 5b and 5c were taken when the wind turbine was operating at 40 rpm and producing 100 kW of power. The wind was from the south-west at  $242^\circ$ , with a velocity of 26 mph. The rotor horizontal axis of rotation was oriented almost due east-west at  $262^\circ$ , or  $20^\circ$  off of the wind direction as indicated by the meteorological tower. The meteorological tower is located about 700 feet southwest of the 100 kW wind turbine. The rotor blade beamwise bending moment ( $M_m$ ) shown in Figure 5a at blade radial station 40 varied from 0. to -130,000 ft-lbs for each rotor revolution. Negative beamwise bending moments cause the rotor blade to deflect out of the plane of rotation toward the tower structure.

Wind speed measurements near the sides of the tower indicate that the wind velocity on the downwind side of the tower is substantially reduced with respect to the free stream wind velocity as a result of air flow blockage by the tower structural members. As the rotor blade passes downwind of the tower, it enters a wind stream of relatively low velocity or the so-called "tower shadow." The blade responds to a combination of (1) the relative absence of wind loads

due to tower shadow and (2) the continual bending moments induced by centrifugal loads due to the rotational speed and the  $7^{\circ}$  blade cone angle. The maximum beamwise bending moment response of the blade occurs at about  $\alpha = 35^{\circ}$ .

The beamwise bending moment at radial station 370 appears to be similar in wave form and in phase with the beamwise bending moment at station 40, as shown in Figure 5a. The wave form and phase for the chordwise bending moment at station 40 is generally similar to that at station 370, as seen in Figure 5a. This implies that the blade is bending similarly to a cantilevered beam. The magnitudes for these mean and cyclic bending moments are summarized in Table I. The blade pitch angle setting varied from  $-10^{\circ}$  to  $-9^{\circ}$  with respect to the chordline at 0.75 r/R. The low speed shaft torque shown in Figure 5b varied between 18,000 ft-lbs and 32,400 ft-lbs, while the power fluctuated from 93 kW to 100 kW.

The tower displacements at the 83 ft. level varied from  $-.15$  to  $+4$  inches along the  $x$  direction as defined in Figure 5c. Tower displacements in the  $y$  direction were small compared to deflections in the  $x$  direction also shown in Figure 5c.

Data from the accelerometers mounted on the bearing support, nearest the rotor blades were recorded as shown in Figure 5c. Fourier analysis of the data taken from the accelerometer measuring vertical accelerations ( $\ddot{Y}$ ) indicates a high 10P (10 cycles per rotor revolution) content. Response from the accelerometer measuring horizontal acceleration ( $\ddot{X}$ ) indicates a combination of tower and nacelle motion when compared with the tower deflections at 83 ft.

The data, shown in Figure 6, was taken when the wind turbine was operating at 40 rpm and zero power. The wind velocity, wind direction and nacelle direction, with respect to the wind direction, were identical to the conditions experienced during operation at design speed and rated power.

As in the powered condition, the beamwise and chordwise bending moment wave forms at blade radial station 40 are similar to the wave forms at station 370 shown in Figure 6. These mean and cyclic blade bending moments are summarized in Table I. It is noted that an increase in blade mean and cyclic bending moments occur when the power is reduced from 100 kW to 0 kW. For example, the beamwise mean bending moment at station 370 increased by 43% when the power was reduced. The large increase in the mean blade beamwise bending moment is due to a decrease in the thrust loading on the blades during operation at zero power. As shown in Figure 6 the blade pitch angle was set at about  $-12.5^{\circ}$  while maintaining 40 rpm at zero power.

### Emergency Feather

During operation at 40 rpm and 0. kW, a liquid level sensor sensed a low hydraulic oil level in the reservoir feeding the hydraulic pump. The hydraulic pump supplies oil to the blade pitch control actuators through an electro-hydraulic servovalve. When a low hydraulic oil supply is sensed, emergency shutdown is initiated and the control system automatically activates a rapid collective change in the blade pitch angle. The blade pitch angle changes from the operating pitch angle ( $0^\circ$ ) to the full feather pitch angle ( $90^\circ$ ). This rapid blade pitch angle change is referred to as an "emergency feather."

The test data shown in Figure 7 indicates that the blade pitch angle changed from  $-6^\circ$  to  $-89.5^\circ$  in about 20 seconds. The rotor speed decreased from 40 rpm to 0 rpm in about 23 seconds.

Maximum beamwise bending moments at station 40 and 370 occurred at 1.7 and 1.4 seconds respectively after initiation of the emergency feather. At station 40, the maximum beamwise bending moment measured was -160,000 ft-lbs and at station 370, -47,000 ft-lbs.

A maximum chordwise bending moment, at station 40, of -96,000 ft-lbs occurred 1.1 seconds after initiation of the emergency feather, with moments approaching this value at 2.8 and 4.8 seconds after initiation. The maximum value for shaft torsion, at 8,000 ft-lbs, occurred at 2.5 seconds after initiation.

### System Response to Rotor Speed Variation

Figures 8a through 8d present a set of circumstances which depict the close interaction between system dynamics and rotor speed. During this phase of operation the wind speed, indicated by the nacelle anemometer, was varying between 22 and 37 mph.

It was difficult for the control system to maintain constant rotor speed as shown in Figure 8a. Power output was constant at 40 kW. As rotor speed increases from 38 rpm to 40 rpm chordwise motion of the rotor blades indicated by the bending moment traces,  $M_n$ , at stations 40 and 370 increased. Beamwise bending response also increases. The right hand half of the beamwise bending moment trace at station 40 shows a large cyclic or asymmetric motion of the rotor blades. This is indicated by the two or three cycles of symmetric response signals, in the station 40 trace. At the same time, the rotor shaft torque,  $M_z$ , shown in Figure 8b, indicates a large oscillatory response to the inplane blade motions each time the rotor speed changes from 38 to 40 rpm. The tower and nacelle also exhibit large response during each occurrence, as shown in Figure 8c.

This condition is illustrative of the importance of dynamic response considerations in the design of large wind turbines. For the

condition cited, a rotor blade chordwise bending moment increase of 50% and rotor shaft torque oscillations with a peak-to-peak magnitude of 1.8 times the design torque are experienced as the machine speed is varied by only 2 rpm. This condition will require the selection of a new rotor operating speed, or some modification of the rotor blades themselves to reduce the chordwise bending response at or near the selected rotor speed. Repeated occurrences of this condition during normal operation of the machine cannot be tolerated. We are currently assessing the various options available to correct this situation.

#### Comparison of Test Data With Analysis

The MOSTAB-WT computer program for analysis of rotor loads and response (ref. 3) was developed for use in the helicopter industry and has been adapted for wind turbine rotor analysis.

Figure 9 presents a comparison of predicted loads obtained from the MOSTAB program and the measured data. The loads predicted by analysis are shown for two tower shadow values,  $\Delta V/V \approx .25$  (mild tower shadow) and 1.0 (maximum tower shadow).

The effects of tower shadow are modeled in the MOSTAB code by treating the shadow as a sector area of lower-velocity air, as depicted in Figure 10. As indicated in Figure 9, tower shadow has a major influence on the beamwise bending load on the blade. At the time of design, tower shadow was represented by a velocity decrement,  $\Delta V/V \approx .25$  over a sector angle of  $18^\circ$ , which is consistent with the data presented in ref. 4.

The recent tests showed blade loads which are significantly higher than those predicted using a velocity decrement of 0.25. Because of these higher loads, additional analysis was conducted in order to determine what velocity decrement is needed to produce these loads. The measured loads can be reproduced analytically by a velocity decrement  $\Delta V/V$  of 0.93.

Recent wind tunnel tests conducted at NASA-Lewis have indicated that tower shadow velocity decrement can equal or exceed this selected value of 0.93 in small local areas downwind of specific tower members, but the wind tunnel data do not support the use of this large a velocity decrement over the entire sector area behind the tower.

The present MOSTAB simulation for loads analysis includes only one blade degree of freedom and no nacelle or tower flexibility. Modification of the MOSTAB computer simulation to include more degrees of freedom in the rotor and the effect of tower and nacelle motion will result in an improved simulation and will likely agree more closely with the measured data.

Work is nearing completion on this revised computer program. When the program is complete, we will have capability for including multiple degrees of freedom in the rotor and the dynamics of the tower, the nacelle, drive train and control system in addition to aerodynamics and performance considerations that we presently have.

#### Concluding Remarks

Testing of the 100 kW wind turbine to date has been limited to a relatively few hours of total run time. However, this initial operation has already resulted in information valuable to the Wind Energy Program.

Early test results have emphasized the importance of tower shadow considerations in rotor and tower designs. The initial designs were based on a tower-shadow velocity decrement of 25 percent, a value consistent with ref. 4. Test results indicated that this tower shadow did not adequately describe the Mod-0 case and that a substantially higher velocity decrement should be used. As a result of impact of tower shadow on blade and tower loads, tower designs that reduce tower shadow should be investigated in design studies, wind tunnel tests, and tests of wind turbines.

## NOMENCLATURE

$M_L$	rotor blade torsion moment (ft-lbs)
$M_m$	rotor blade beamwise moment (ft-lbs)
$M_n$	rotor blade chordwise moment (ft-lbs)
$M_x, M_y$	low speed shaft bending moments (ft-lbs)
$M_z$	low speed shaft torsion moment
$V$	wind speed (miles per hour)
$\Delta V$	change in wind velocity (miles per hour)
$V_{oc}$	free stream wind velocity (miles per hour)
$X$	horizontal axis normal to low speed shaft
$Y$	vertical axis normal to low speed shaft
$Z$	horizontal axis parallel to low speed shaft
$\tau$	rotor azimuthal position (degrees)
$\theta_n$	nacelle angle measured from magnetic north (degrees)
$\theta_w$	wind angle measured from magnetic north (degrees)
$\phi_n$	nacelle angle at yaw relative to wind vector

ORIGINAL PAGE IS  
OF POOR QUALITY

## REFERENCES

1. Donham, R. E.; Schmidt, Jaap; and Linscott, B.: 100-kW Hingeless Metal Wind Turbine Blade Design, Analysis and Fabrication. 31st Annual National Forum of the American Helicopter Society. Preprint No. S-998, Amer. Helicopter Soc., 1975.
2. Puthoff, R. J.: Fabrication and Assembly of the ERDA/NASA 100-Kilowatt Experimental Wind Turbine. NASA TM X-3390, 1976.
3. Hoffman, J. A.; and Holchin, B. W.: Modifications to MOSTAB For Wind Turbine Applications. Mechanics Research Inc. Report 2711, July 1974.
4. Ammann & Whitney, Consulting Engineers: Wind Tunnel Tests on Models of Kennedy Space Center Structures. Contract No. DA-08-176-Eng (NASA)-341, Sept. 1967.

SUMMARY OF MEAN AND CYCLIC  
LOAD FLAKE BENDING MOMENTS

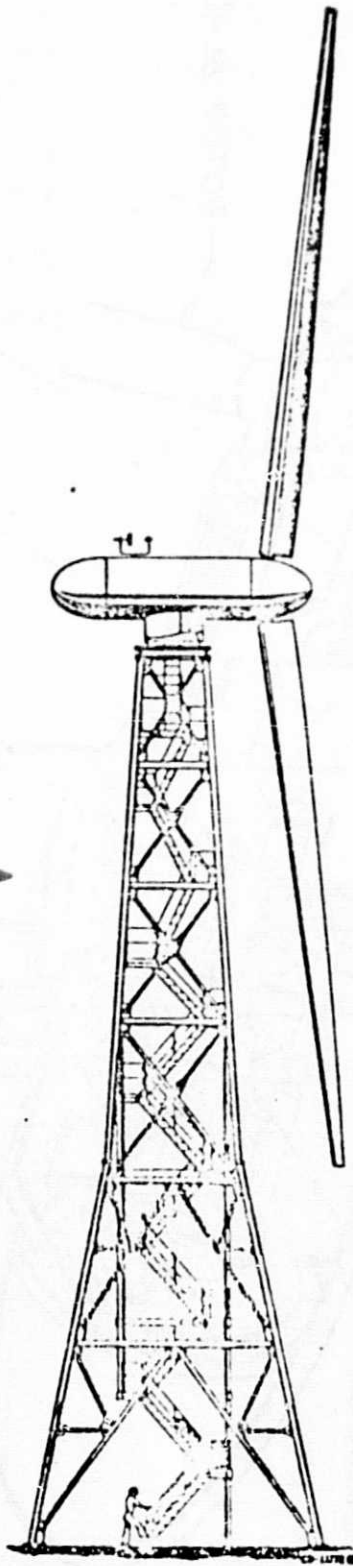
	SHEET LOCATION.	40 RPM - 100 KW		40 RPM - 0 KW.	
		MEAN	CYCLIC	MEAN	CYCLIC
FLAKEWISE	40	(-65,000)	(±65,000)	(-110,000)	(±70,000)
BLANKING	370	(-11,250)	(±18,750)	(-26,250)	(±18,750)
CHUCKWISE	40	(-18,000)	(±54,000)	(-18,000)	(±66,000)
BENDING	370	(-2000)	(±14,000)	(-4000)	(±20,000)

UNITS : NEWTON-METERS (POUND-FT)

TABLE 1

PRECEDING PAGE BLANK NOT FILMED

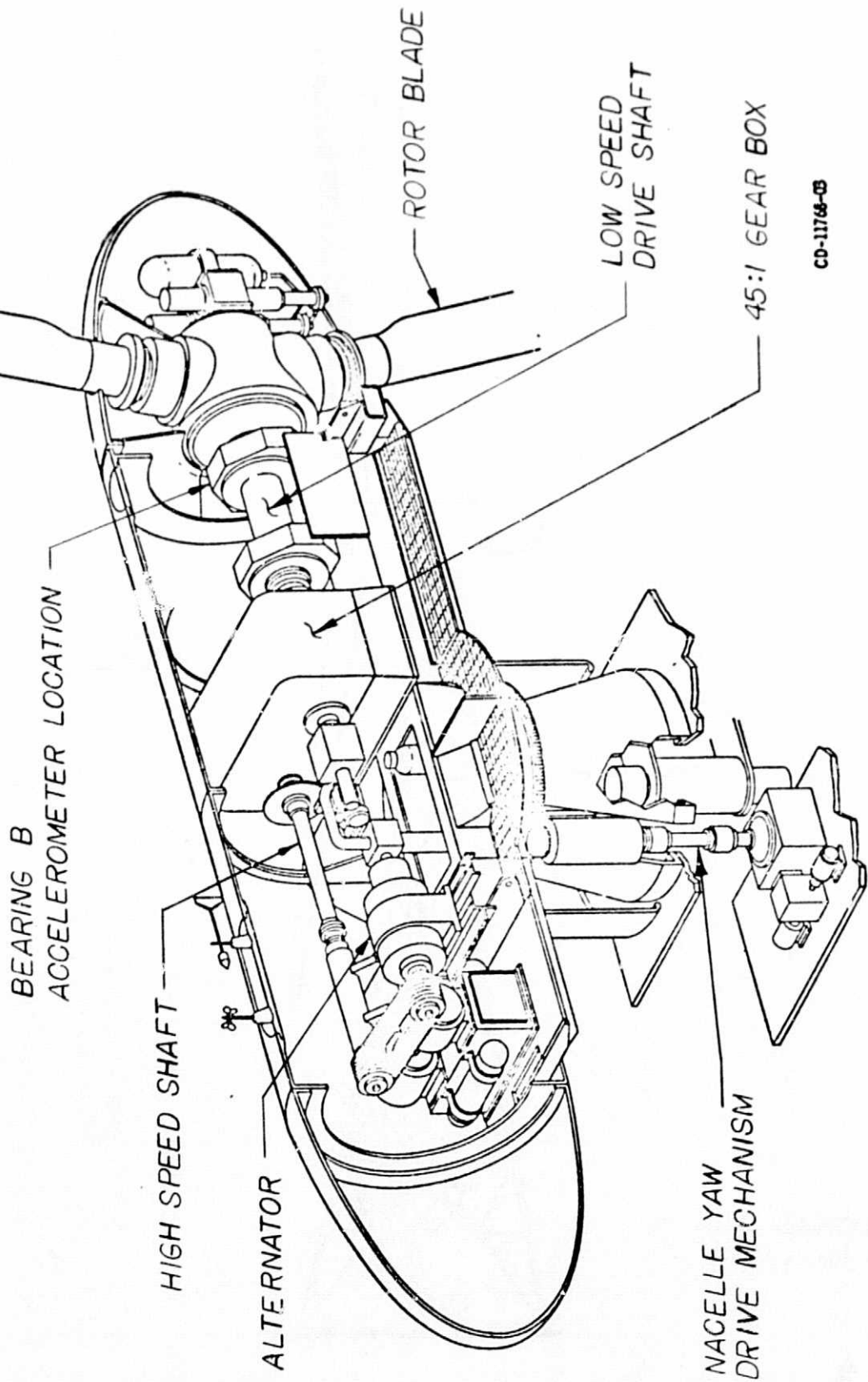
WIND →



ORIGINAL PAGE IS  
OF POOR QUALITY

Figure 1 100 kW Mod-0 Wind Turbine

# 100KW EXPERIMENTAL WIND TURBINE GENERATOR



CO-11768-03

FIGURE 2

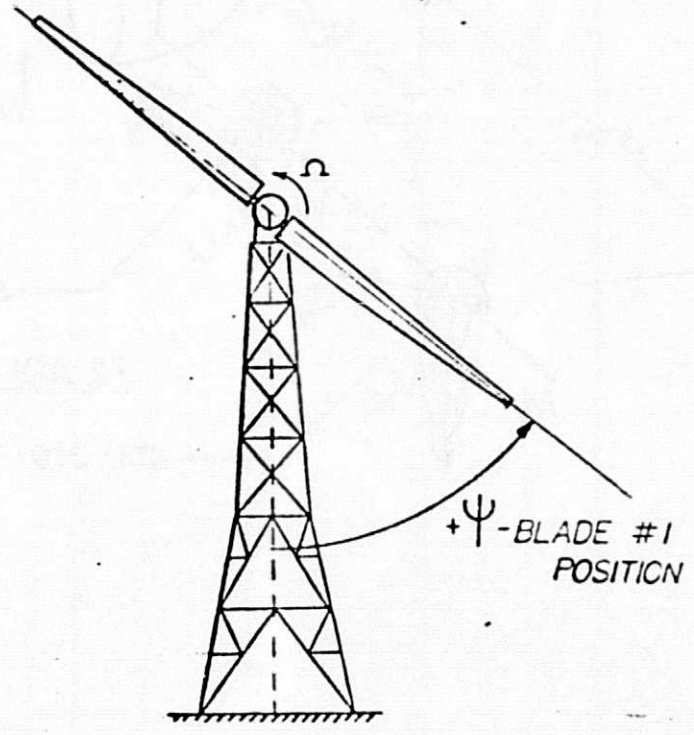
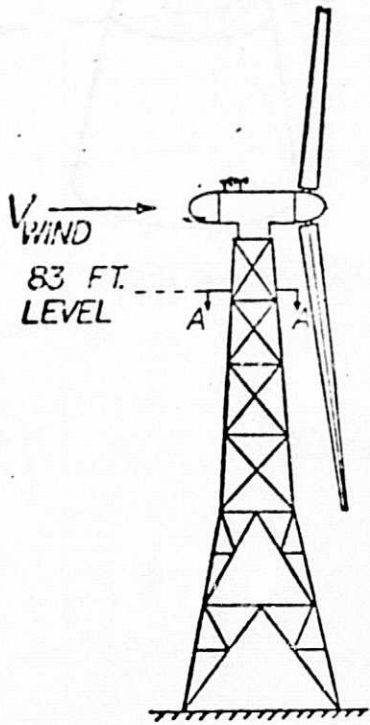
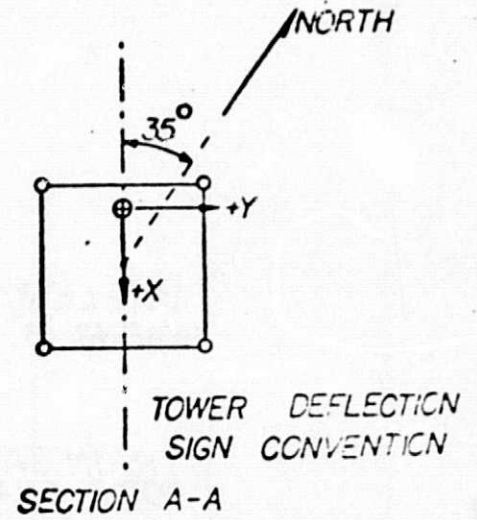
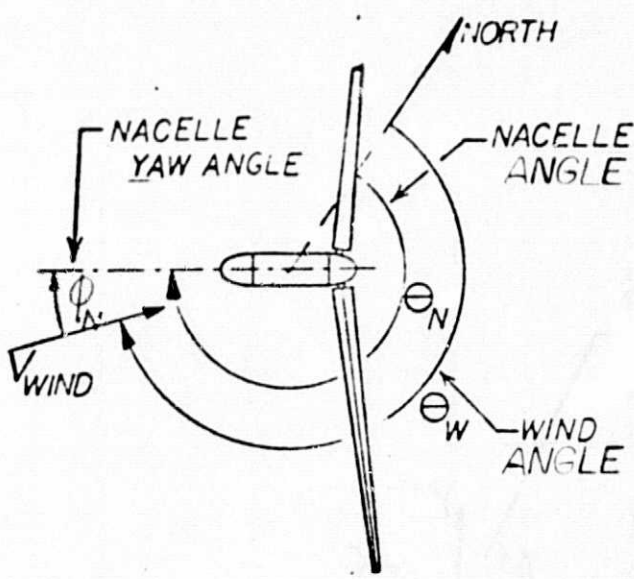


FIGURE 3

ORIGINAL PAGE IS OF POOR QUALITY

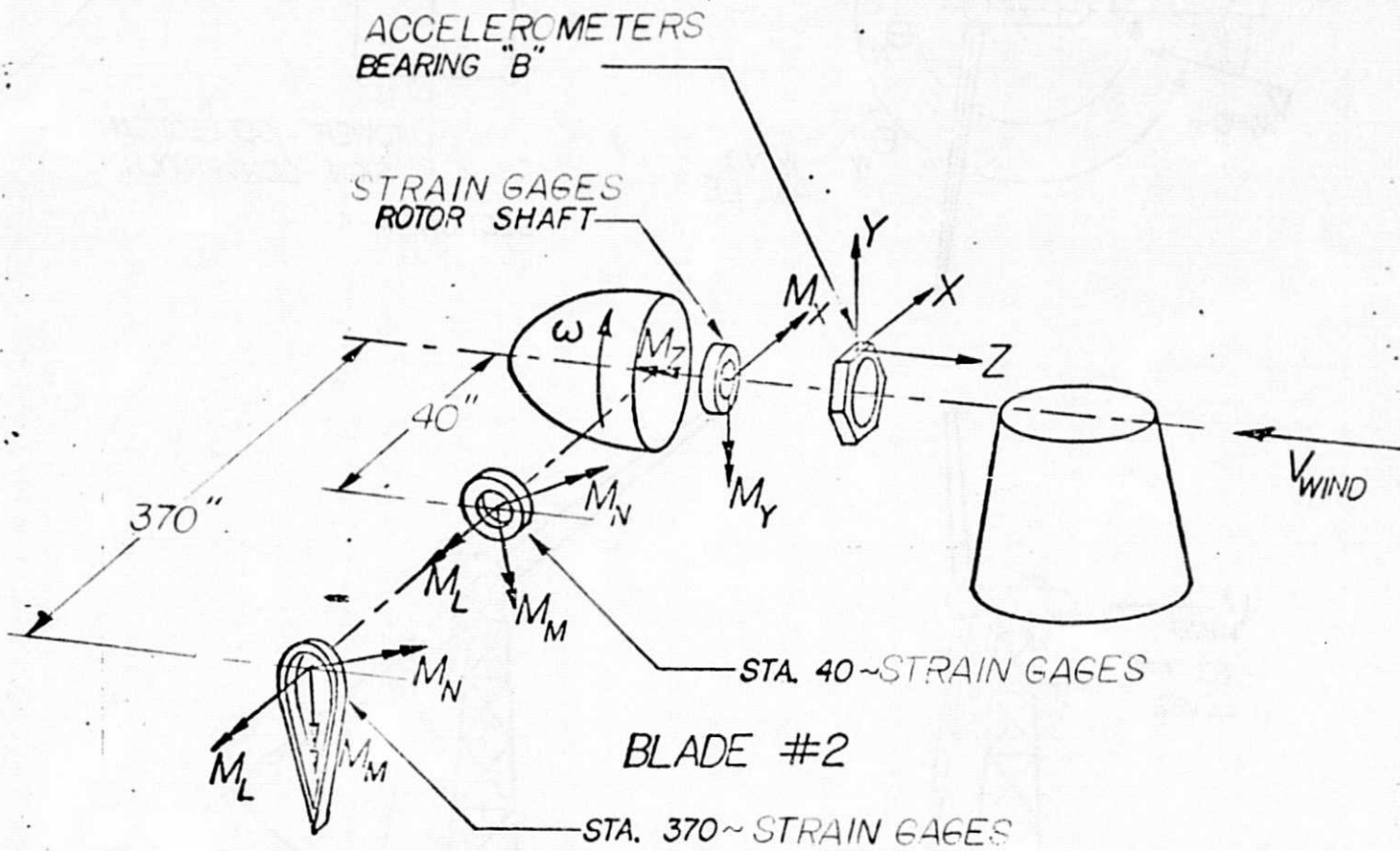


FIGURE 4

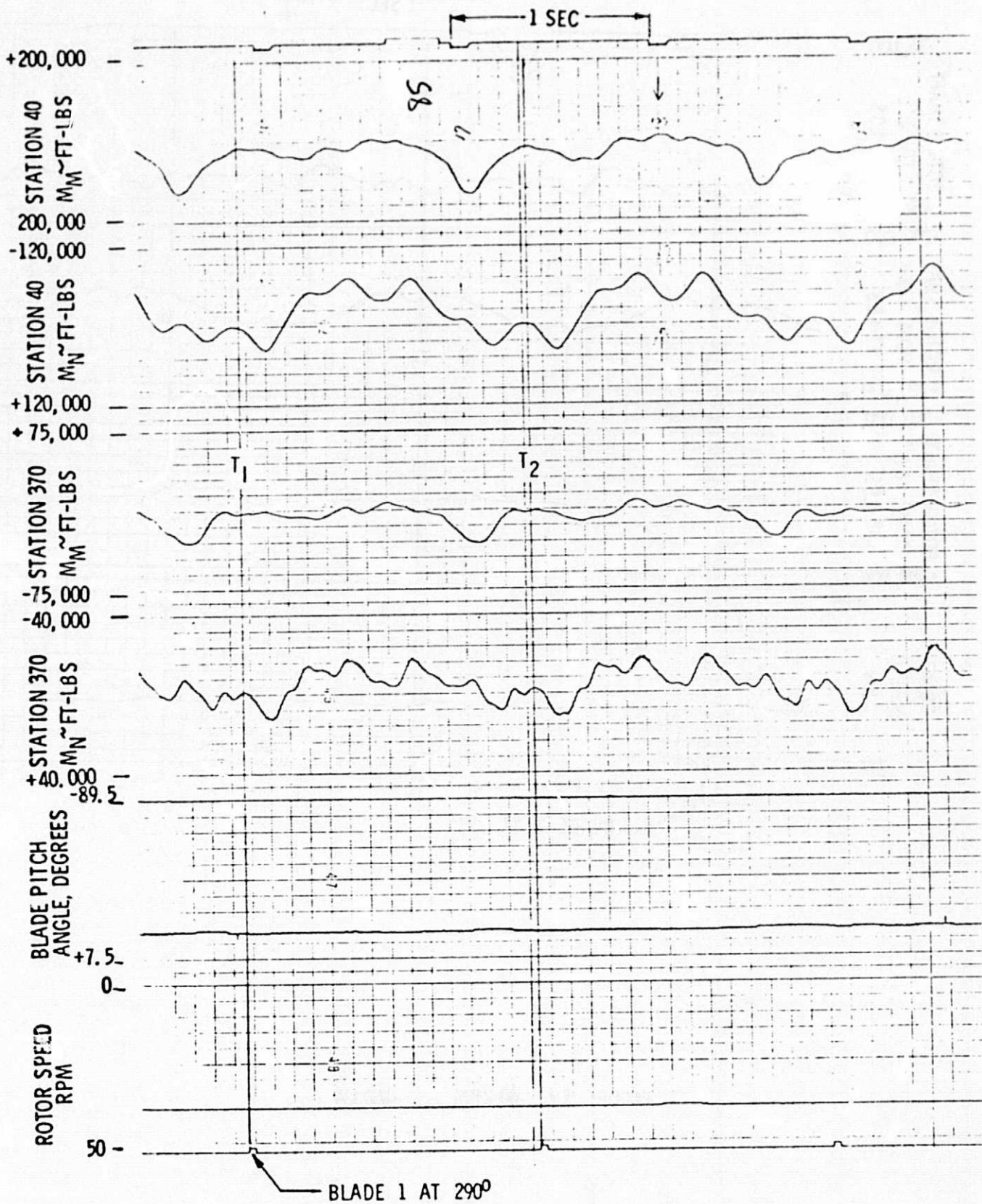


FIGURE 5a 40 RPM , 100 kW

ORIGINAL PAGE IS  
OF POOR QUALITY

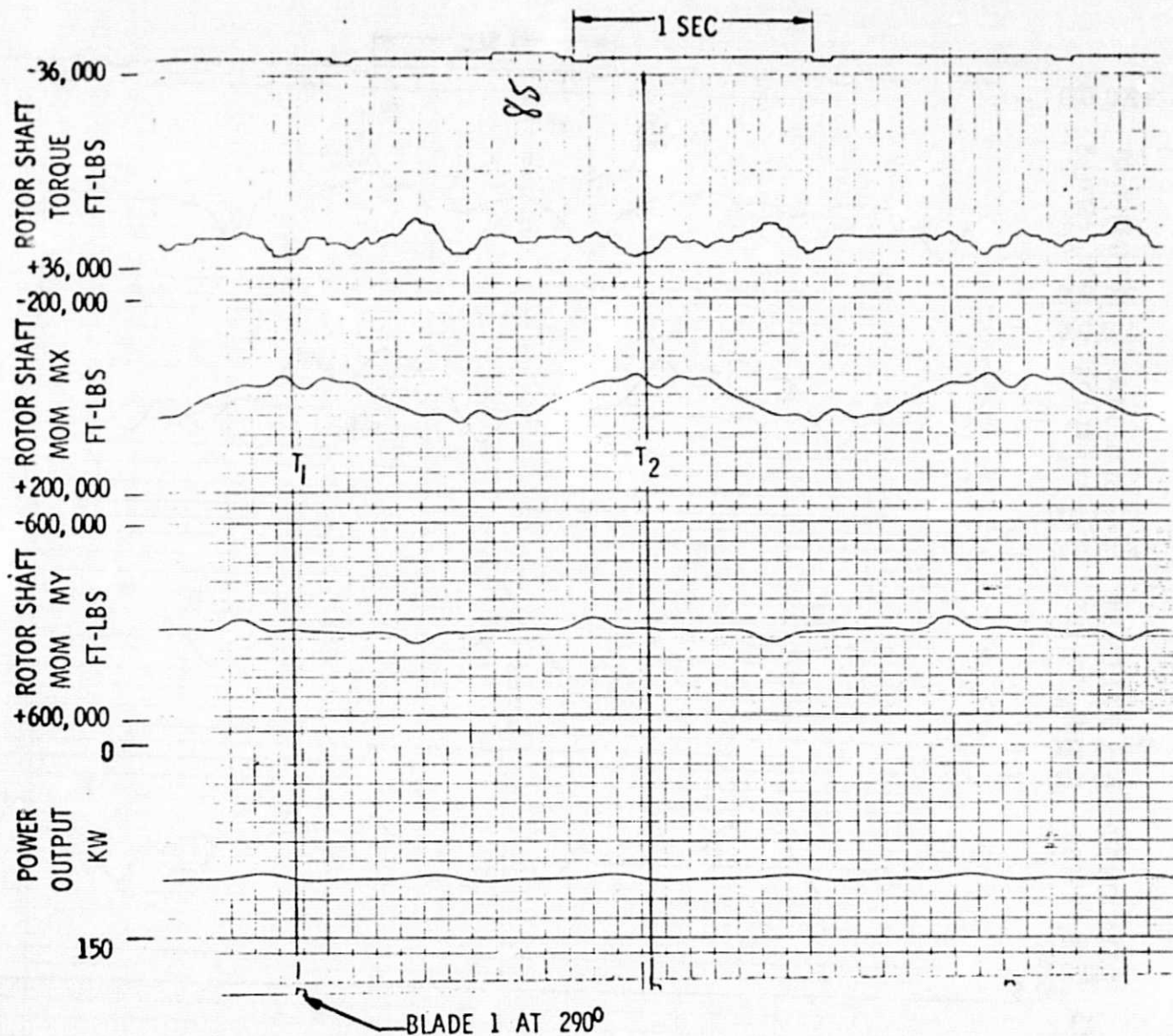


FIGURE 56 40 RPM , 100 kW

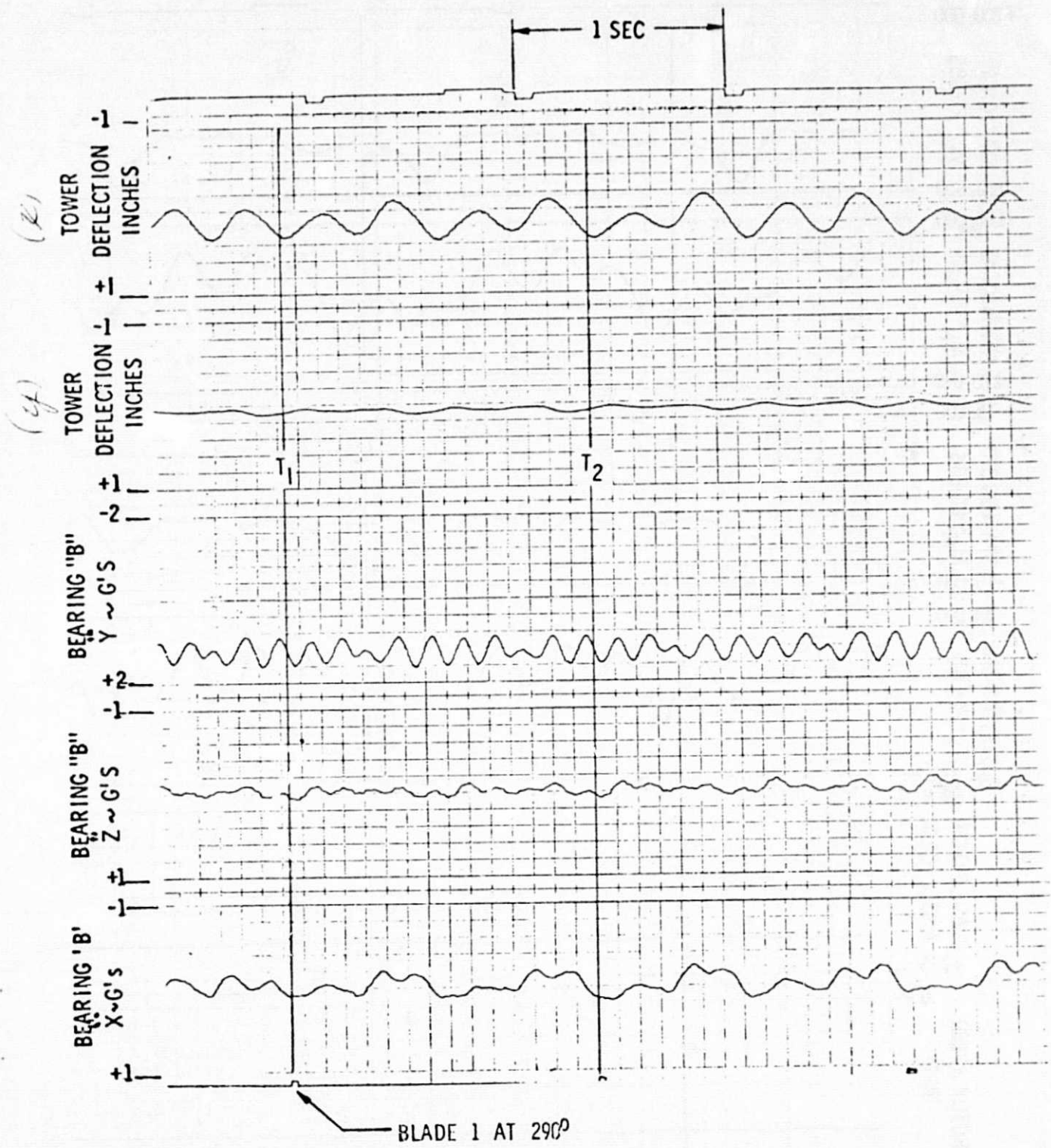


FIGURE 5c 40 RPM , 100 kW

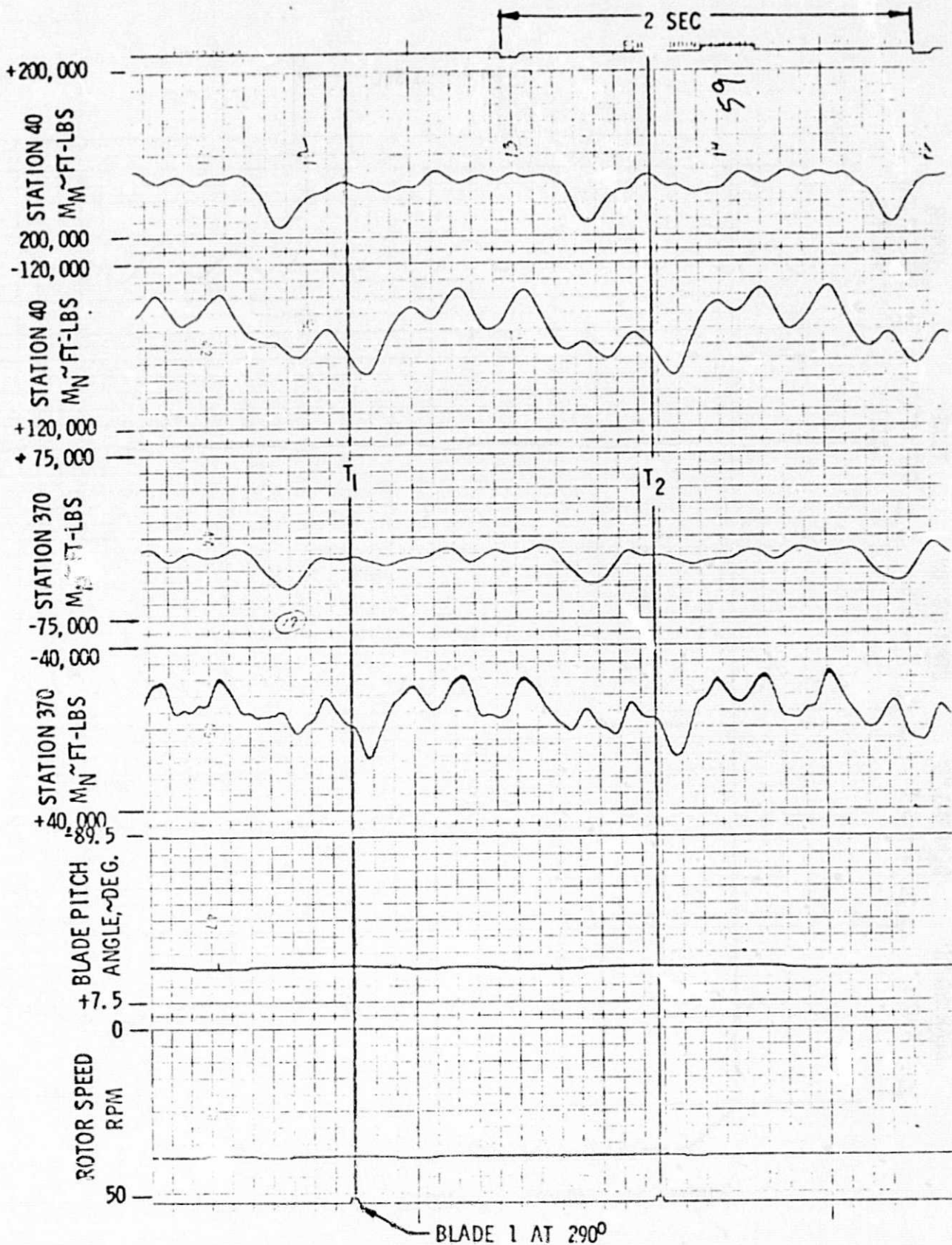


FIGURE 6 40 RPM , 0 POWER

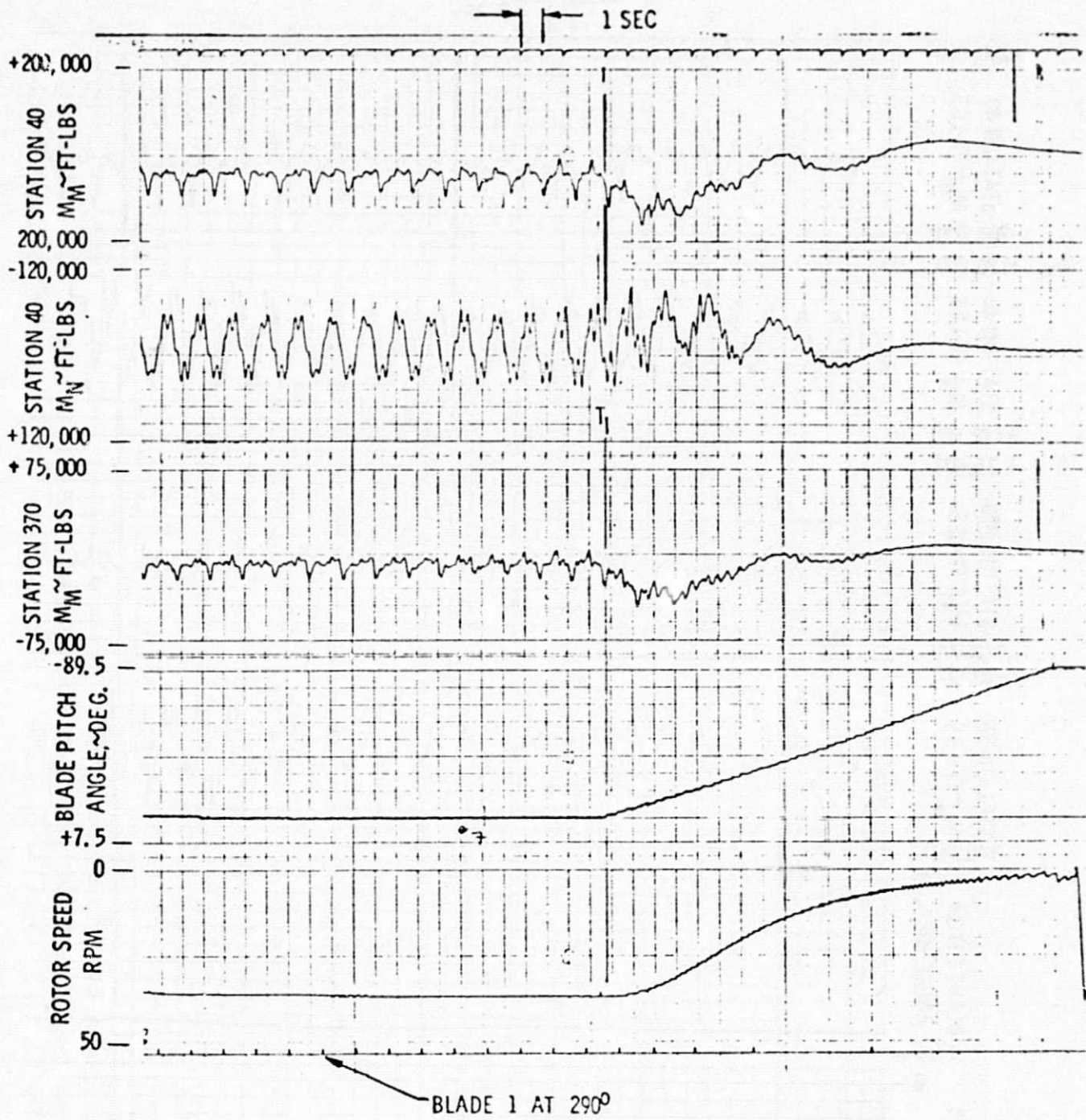


FIGURE 7 EMERGENCY FEATHER

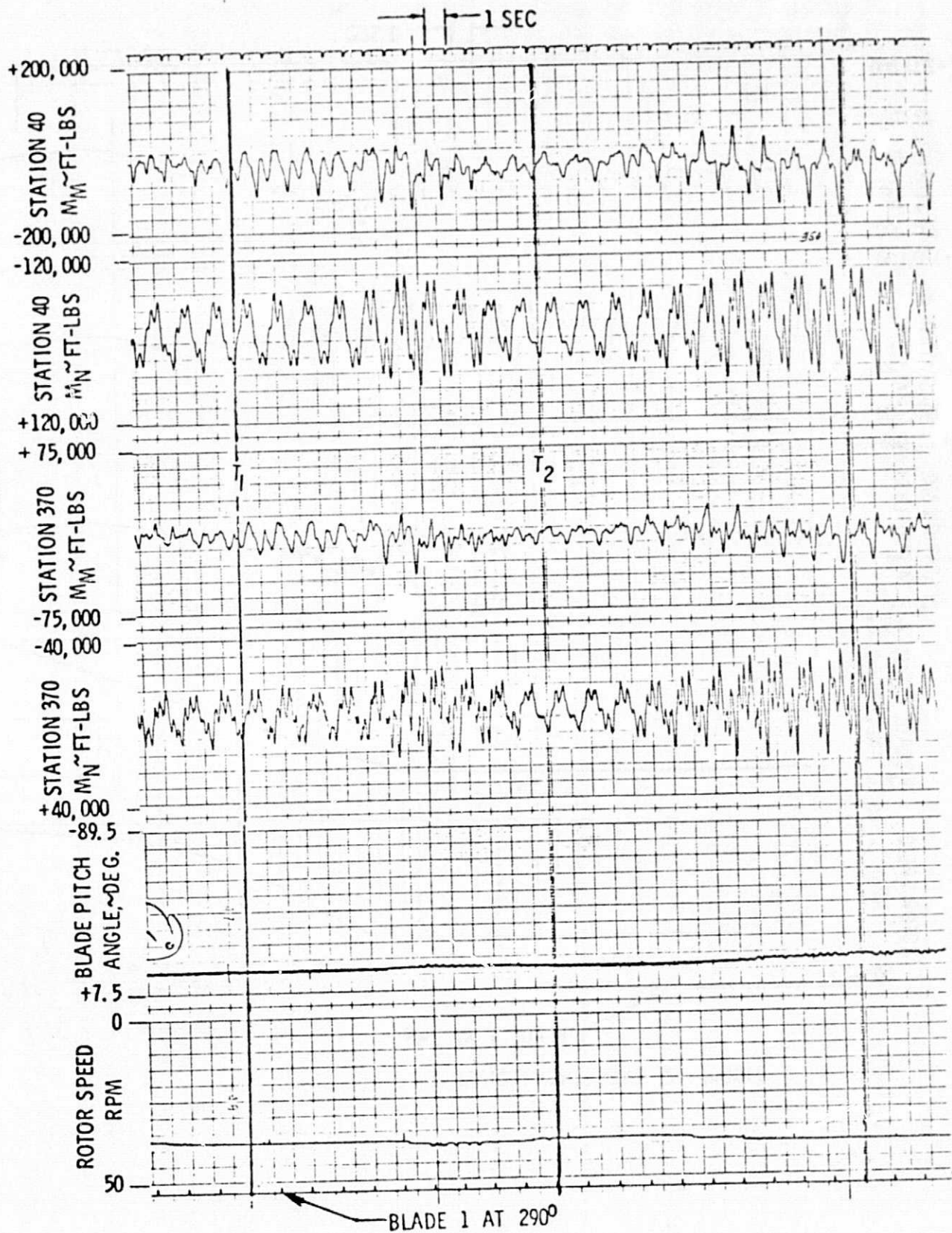


FIGURE 3a GUST RESPONSE (W/SHAFT OSCILLATION)

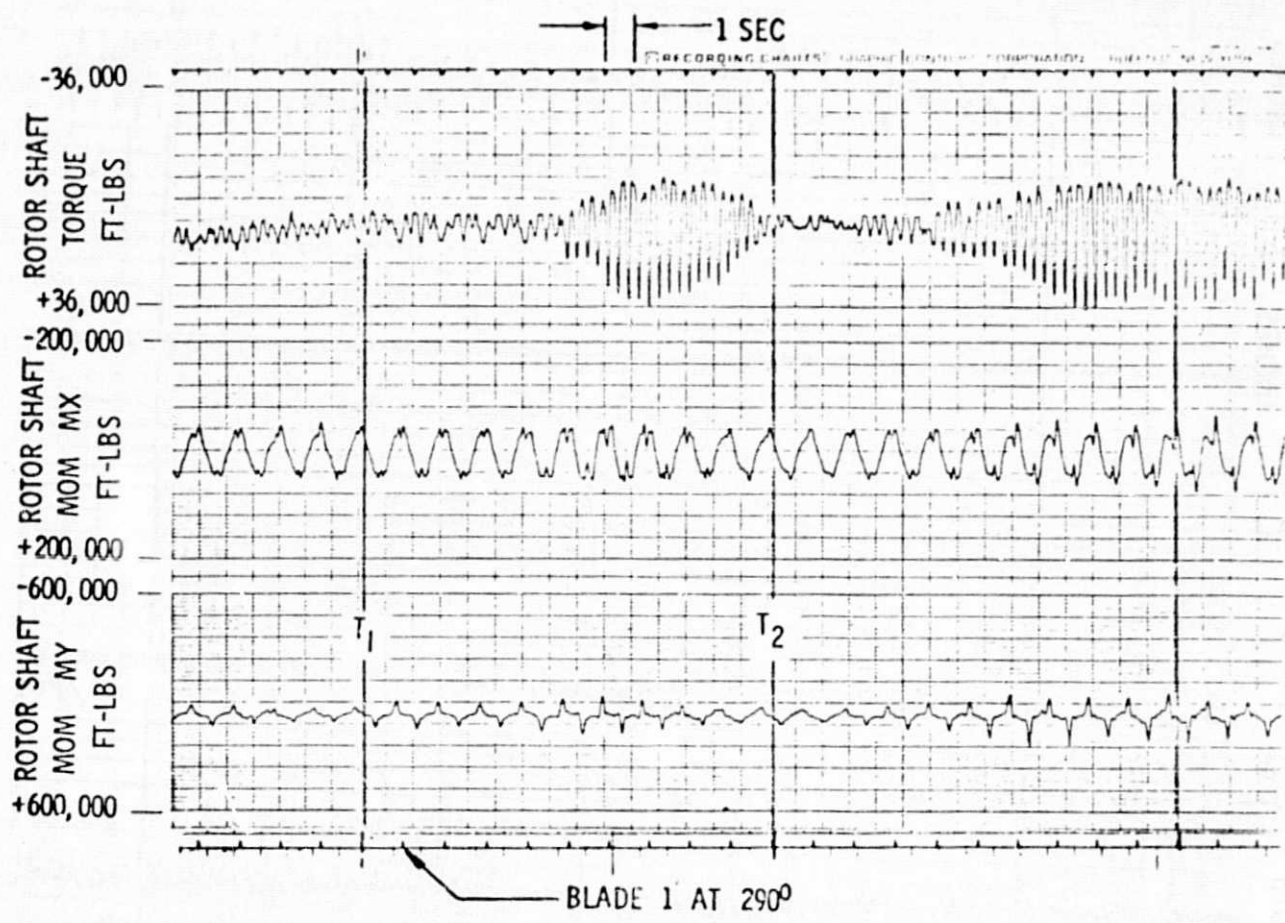


FIGURE 8 b GUST RESPONSE (W/SHAFT OSCILLATION)

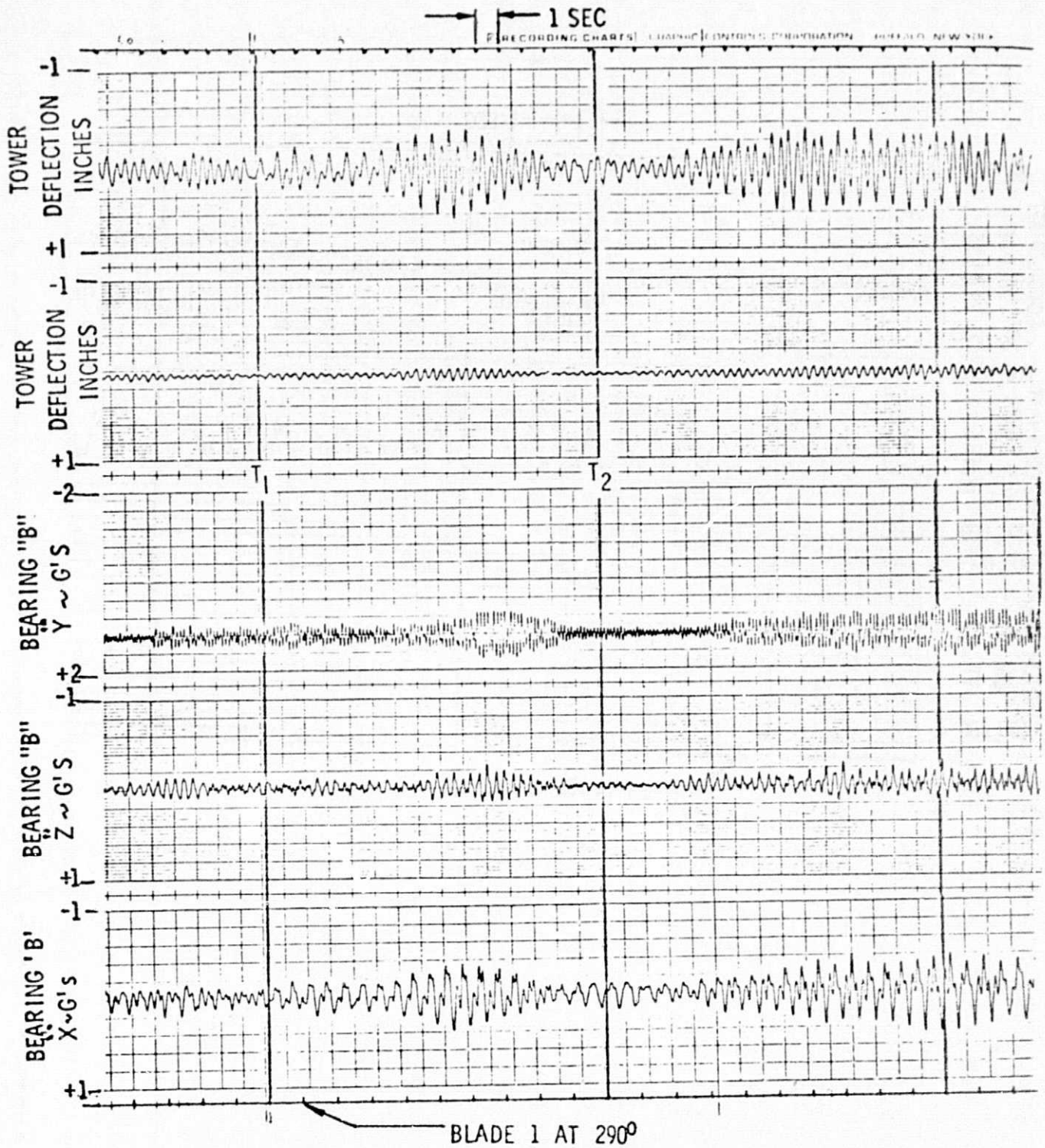


FIGURE 8c GUST RESPONSE (W/SHAFT OSCILLATION)

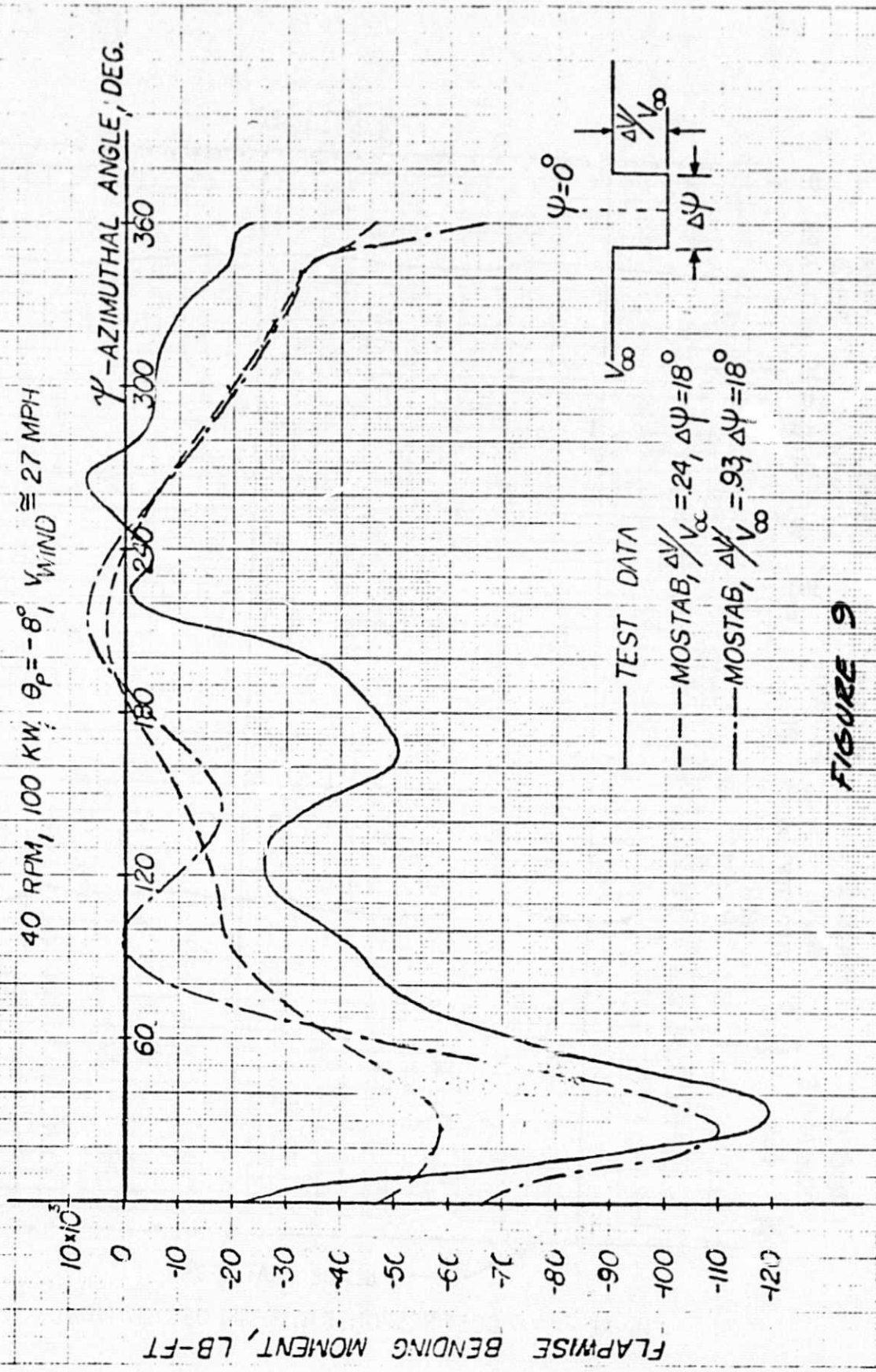


FIGURE 8d GUST RESPONSE (W/SHAFT OSCILLATION)

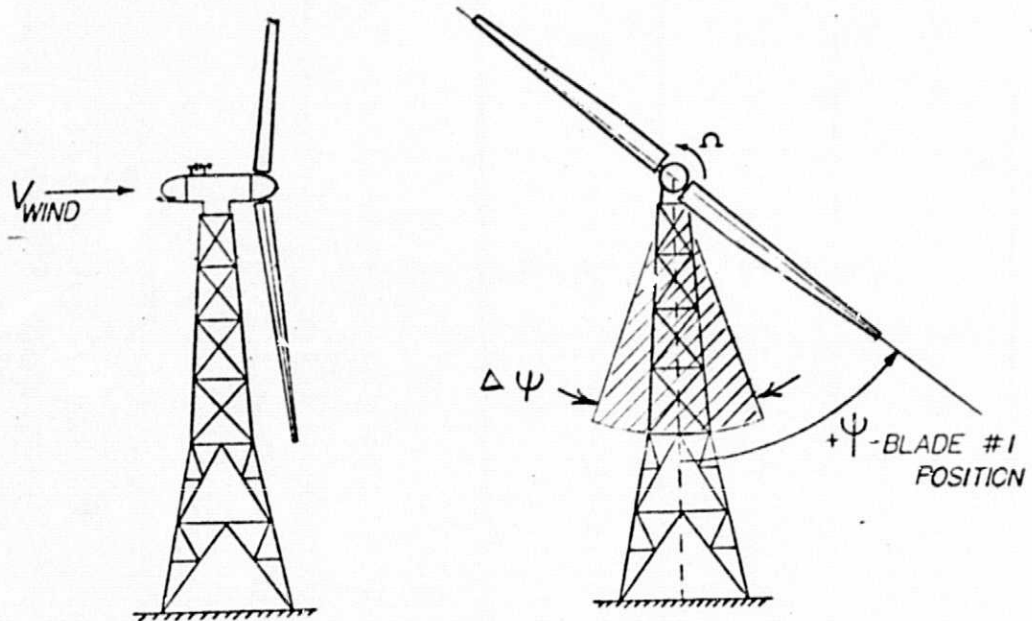
**FIGURE 9** BLADE LOAD COMPARISON

MOSTAB PREDICTIONS VS TEST DATA

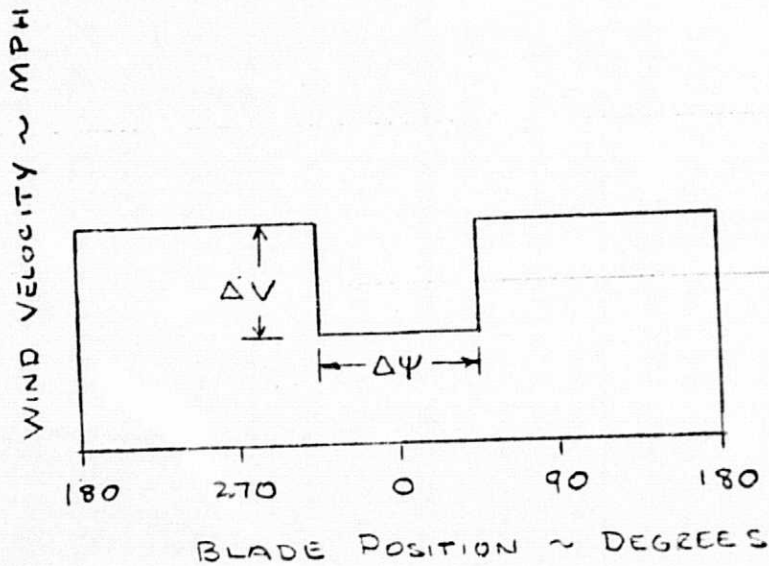
40 RPM, 100 KW;  $\theta_p = -8^\circ$ ,  $V_{WIND} \approx 27$  MPH



**FIGURE 9**



$\Delta\Psi$  - SECTOR OVER WHICH WIND VELOCITY IS RETARDED  
 $\Delta V$  - VELOCITY DECREMENT BEHIND TOWER



ORIGINAL PAGE IS  
 OF POOR QUALITY

FIGURE 10. TOWER SHADOW MODEL